

Ab initio molecular-dynamics study of highly nonideal structural and thermodynamic properties of liquid Ni-Al alloys

M. Asta,¹ V. Ozoliņš,² J. J. Hoyt,³ and M. van Schilfgaarde²

¹*Department of Materials Science and Engineering, Northwestern University, Evanston, Illinois 60208*

²*Sandia National Laboratories, Livermore, California 94551-0969*

³*Sandia National Laboratories, Albuquerque, New Mexico 87185-1411*

(Received 19 March 2001; revised manuscript received 1 May 2001; published 22 June 2001)

Atomic and electronic structure, and diffusion coefficients in liquid Ni-Al alloys, have been calculated by *ab initio* molecular-dynamics simulations. The chemically short-range ordered structure of liquid Ni₂₀Al₈₀ measured by neutron scattering is well reproduced in these simulations. We calculate a significant electronic contribution ($\Delta S_{el} = -0.4 k_B/\text{atom}$) to the formation entropy of NiAl at 1900 K, originating from a simultaneous narrowing and shifting of the Ni *d* band to higher binding energies accompanying alloying with Al. This value of ΔS_{el} , combined with an estimate for the configurational entropy based on calculated radial distribution functions and a nonadditive hard-sphere model, accounts for the large negative excess entropy of mixing measured in liquid Ni-Al alloys.

DOI: 10.1103/PhysRevB.64.020201

PACS number(s): 61.25.Mv, 71.22.+i, 65.20.+w, 65.40.Gr

Transition-metal-aluminum (TM-Al) alloys form a technologically important class of materials that are of fundamental interest due to the structural complexity associated with many of their intermetallic phases. While the properties of crystalline TM-Al alloys have been topics of numerous theoretical and experimental studies, far less attention has been devoted to noncrystalline phases and liquids in particular. TM-Al alloys are the basis for a variety of bulk metallic glass forming systems, and efforts to optimize the properties of these materials have led to increasing interest in understanding the thermodynamic and kinetic properties of the liquid phases from which they form. The Ni-Al system is of particular interest in this context since properties in the liquid phase are relatively well characterized experimentally yet uncertainties persist in theoretical models of bonding, structure, and thermodynamics in these alloys.

The structure of liquid Ni₂₀Al₈₀ was measured by Maret *et al.*¹ using isotope substitution neutron scattering to extract each of the three independent structure factors at $T = 1330$ K. A significant degree of chemical short-range order (SRO) was measured in these liquids, as characterized by a pronounced peak in the chemical-chemical Bhatia-Thornton structure factor.² Consistent with the tendency to form chemical SRO, the solution thermodynamic properties of liquid Ni-Al alloys are highly nonideal. Specifically, the excess entropy of mixing (ΔS_{xs} , the difference between the actual and ideal entropies of mixing) is measured to be as large as $-1.6 k_B/\text{atom}$.^{4,5} Within a model-pseudopotential formalism combined with thermodynamic perturbation theory, Landa and co-workers⁶ studied the origin of the highly nonideal thermodynamic properties in NiAl and suggested that the large values of the excess entropy of mixing could be attributed to two effects: (i) a large negative deviation in liquid alloy atomic volumes from Vegard's law, leading to a sizeable packing entropy^{38–40} contribution to ΔS_{xs} , and (ii) a charge transfer effect whereby the Ni *d* band is filled upon alloying with Al, leading to a reduction in the electronic density of states at the Fermi level and a signifi-

cant negative *electronic entropy* contribution to ΔS_{xs} .⁷ More recently, Pasturel and co-workers^{8–10} have emphasized the importance of (iii) chemical SRO in modeling the thermodynamic properties of liquid Ni-Al alloys. Effects (i)–(iii) have not yet been modeled within a consistent theoretical framework, and the relative magnitudes of these different contributions to the excess thermodynamic properties therefore remains unclear. To further clarify the microscopic origins of the highly nonideal solution thermodynamic properties in this system we have undertaken a study of liquid Ni-Al based upon *ab initio* molecular-dynamics (AIMD) simulations.

AIMD simulations of liquid Ni-Al alloys were performed using the *ab initio* total-energy and molecular-dynamics program VASP (Vienna *ab initio* simulation package) developed at the Institut für Material-physik of the Universität Wien.^{11,12} The VASP code makes use of ultrasoft pseudopotentials,¹³ and an expansion of the electronic wave functions in plane waves. This approach has been applied widely in AIMD simulations of liquid metals and alloys (see, for example, Refs. 14–24). Simulations were performed in the local density approximation²⁵ using a plane-wave cutoff of 242 eV. Γ -point sampling was used in simulations for Ni₂₀Al₈₀ liquids at 1300 K, whereas in the calculations of electronic densities of states and electronic entropy for Al, Ni, and NiAl at 1900 K use was made of a $2 \times 2 \times 2$ and $4 \times 4 \times 4$ Monkhorst-Pack *k*-point meshes.²⁶ Electronic levels were occupied according to Fermi-Dirac statistics with the electronic temperature set equal to that of the ions. All of the simulations reported here were performed at experimentally measured liquid densities. Newton's equations of motion were integrated using the Verlet algorithm²⁷ with a time step of 3 fs, and use was made of a Nosé thermostat²⁸ to control temperature.

In Fig. 1 we compare our calculated and measured¹ structure factors for a Ni₂₀Al₈₀ liquid. Figure 1(a) features a comparison between AIMD results for the Bhatia-Thornton² correlation functions, with results extracted from structure

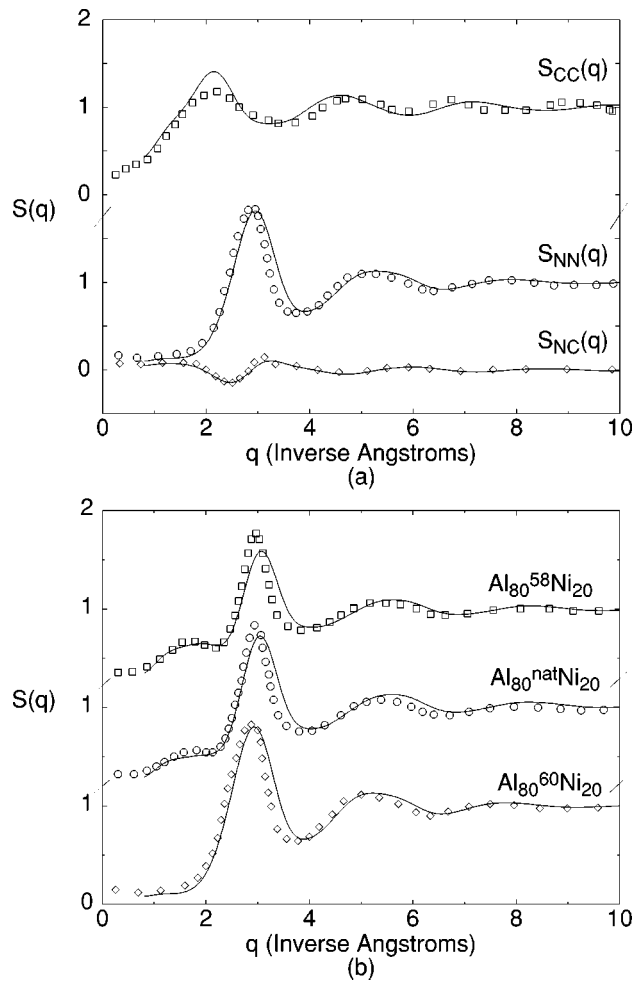


FIG. 1. Calculated (solid lines) and measured (circles) (Ref. 1) Bhatia-Thornton structure factors (a) and total structure factors (b) for liquid $\text{Ni}_{20}\text{Al}_{80}$.

factors measured as a function of Ni isotope concentration.¹ Since the extraction of partial structure factors from experimental data can be subject to uncertainties, we also compare calculated and measured values for *total* structure factors in Fig. 1(b). In both figures calculated results were obtained by Fourier transforming partial-pair correlation functions derived from 256 atom simulations performed at 1300 K. Radial distribution functions were averaged during a simulation lasting 6.9 ps which followed a 1.3 ps equilibration phase beginning with atomic positions extracted from embedded-atom-method (EAM) based Monte Carlo simulations.³² The agreement between experiment and theory displayed in Fig. 1(a) is seen to be good for both the number-number and number-chemical correlation functions, $S_{NN}(q)$ and $S_{NC}(q)$. The AIMD simulations also reproduce the pronounced peak in the chemical-chemical structure factor (S_{CC}), indicative of chemical SRO in the liquid. The first peak in the calculated $S_{CC}(q)$ is slightly larger than measurements suggesting a higher degree of chemical SRO in the AIMD simulations. Overall the level of agreement is comparable to that obtained in a previous molecular-dynamics study based upon tight-binding potentials by Phuong *et al.*³ The level of agreement between experiment and theory for total structure factors dis-

TABLE I. Nearest-neighbor distances (R), chemical SRO parameters (α), and diffusion coefficients (D_{Ni} and D_{Al}) for $\text{Ni}_{20}\text{Al}_{80}$ at $T=1300$ K. Nearest-neighbor spacings are given in \AA , while diffusion coefficients are in units of $10^{-4} \text{ cm}^2 \text{ s}^{-1}$.

	$R(\text{NiNi})$	$R(\text{NiAl})$	$R(\text{AlAl})$	D_{Ni}	D_{Al}
AIMD	2.67	2.41	2.73	0.24 ± 0.02	0.42 ± 0.04
Expt. ^a	2.63	2.54	2.82		
EAM ^b	2.52	2.54	2.74	0.75	0.83
EAM ^c	2.50	2.52	2.75	0.86	0.90
EAM ^d	2.56	2.44	2.77	0.52	0.79
TB ^e	2.55	2.55	2.78		

^aExperimental measurements (Ref. 1).

^bVoter and Chen (Ref. 29) EAM potentials.

^cFoiles and Daw (Ref. 30) EAM potentials.

^dLudwig and Gumbsch (Ref. 31) EAM potentials.

^eTight-binding (Ref. 3) potentials.

played in Fig. 1(b) is also found to be quite reasonable. Specifically, the prepeak features measured experimentally are well characterized. Computed positions for the first peak are shifted to slightly higher values of q , suggesting that the bond lengths are underestimated on average by the AIMD calculations relative to experiment.

Nearest-neighbor bond lengths, obtained from the position of the first peak in each of the partial pair correlation functions, are reported in Table I. While the AIMD calculated values show quantitative differences (as large as 4%) compared to experimental results, they capture the trend that the shortest bond length is between *unlike* neighbor bonds (Ni-Al).³³ It is interesting to note that in Table I the AIMD calculated NiAl bond length (2.41 \AA) is significantly smaller than the values of $R(\text{NiAl})$ obtained in all of the previous classical simulation studies,^{3,32} with the exception of the result based on the EAM potentials developed by Ludwig and Gumbsch³¹ which were the only set fit to a data base including first-principles calculated energetics for Ni-Al intermetallic compounds.

In Table I are listed values of the Ni and Al diffusion coefficients (D_{Ni} and D_{Al}) in liquid $\text{Ni}_{20}\text{Al}_{80}$ obtained from AIMD and classical EAM simulations³² at 1300 K. Values of D_{Ni} and D_{Al} have been calculated from MD simulations in the standard manner from the long-time slope of the mean square displacement: $\langle |\mathbf{r}_i(t_0+t) - \mathbf{r}_i(t_0)|^2 \rangle \rightarrow 6D_{it}$, as $t \rightarrow \infty$.³⁴ The AIMD diffusion coefficient for Ni is nearly a factor of two lower than that computed for Al, and both D_{Al} and D_{Ni} values calculated from EAM are substantially higher than the *ab initio* results.

Electronic densities of states (DOS) for liquid NiAl, and elemental liquid Al and Ni, at 1900 K are plotted in Fig. 2. These results were obtained by averaging over DOS generated from ten snapshots taken during the course of 3 ps MD simulations for equilibrated 64-atom liquid structures. The most pronounced feature of the results shown in Fig. 2 is the narrowing of the Ni d -band in the alloy and its shift to higher binding energies, relative to elemental liquid Ni. To explain this feature of the electronic DOS in liquid NiAl, we con-

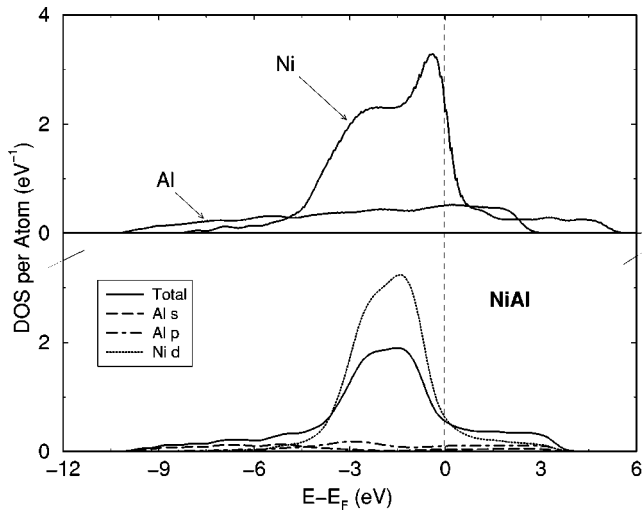


FIG. 2. Calculated electronic densities of states for liquid NiAl and elemental Ni and Al at 1900 K. The thick and thin lines in the bottom panel correspond to total and partial densities of states, respectively.

sider the much simpler bcc $B2$ ordered alloy. The main features of the liquid DOS are replicated there, and the simple interpretation accessible to the $B2$ alloy will carry over to the liquid. For interpretation we employ the method of linear muffin-tin orbitals (LMTO) in the atomic spheres approximation (ASA),³⁵ which partitions space by circumscribing spheres around each nucleus with a radius R_s chosen to match the atomic volume. The ASA is particularly useful here because it provides an easily understood common reference potential with which to align bands of the separate compounds, as we now describe. In elemental Ni and Al, it is evident that each sphere is neutral; consequently at R_s we choose the electrostatic potential to be zero, which fixes the reference in those cases. In the $B2$ alloy, the potential at R_s is the Madelung potential. ASA calculations show a charge transfer of 0.4 electrons from the Al to the Ni spheres, which results in a Madelung potential of ± 8 meV. This shift is so small that we can neglect it. For this reference, the Fermi level of fcc Al and Ni were calculated to be -0.080 eV and -1.011 eV, respectively (each calculated at its own equilibrium volume). Thus on formation of the alloy charge shifts from the Al to the more electronegative Ni, as we noted above. In elemental Ni the d DOS overlaps the Fermi energy (E_F), with about 9.5 states occupied and 0.5 states above E_F , while in liquid and $B2$ NiAl the d states are shifted deeper relative to E_F , as Fig. 2 shows. This net shift is a result of two shifts occurring simultaneously. The Ni d center of gravity shifts upwards about 1.4 eV (owing largely to an increase in atomic volume), while at the same time E_F rises to 0.8 eV (a shift of 1.8 eV relative to elemental Ni); these combine for downward shift of 0.4 eV for $B2$ NiAl in the band center of gravity. Second, there is a narrowing of the NiAl d bands relative to elemental Ni. In part this can be ascribed to a volume effect: well known canonical band theory³⁶ predicts that, in the absence of mixing with s and p states the bandwidth scales as $\Omega^{-5/3}$ with Ω the atomic volume. In the present case canonical theory accounts for a 22

percent narrowing of the bands. Further narrowing is explained by the fact that Ni has fewer neighbors of like kind in the alloy, thus reducing the d bandwidth.

As a consequence of the narrowing and shifting of the Ni d -band upon alloying, the DOS near E_F in liquid NiAl is substantially reduced relative to what would be expected from a composition-weighted average of the density of states for the elemental constituents. These results therefore suggest a large electronic contribution to the entropy of formation of liquid NiAl alloys, as proposed previously.^{6,10} Specifically, from the standard expression for the electronic entropy in the independent electron approximation,³⁷ integrated over the DOS generated from ten liquid structures each for Al, Ni, and NiAl at 1900 K, we compute an electronic formation entropy for liquid NiAl equal to $\Delta S_{el} = -0.42 \pm 0.01$ k_B /atom (where the quoted error estimate represents the standard deviation computed from ten snapshots).

With the above calculated value of ΔS_{el} we can analyze in further detail the origin of the large excess mixing entropy measured for liquid Ni-Al alloys. In addition to the electronic contribution discussed above, we follow Pasturel *et al.*⁷ and estimate the magnitude of the configurational entropy within a hard-sphere model. In the present case we consider a nonadditive hard-sphere model of mixtures to account for the fact that Ni-Al bondlengths are calculated to be much less than the average of those for like-atom neighbors (see Table I). We make use of an analytical expression derived recently within first-order perturbation theory by Ali *et al.*⁴¹ In this framework, the excess configurational entropy is written in the form: $\Delta S_{HS} = \Delta S_{gas} + \Delta S_p + \Delta S_{na}$, where ΔS_{gas} is the ideal gas contribution, ΔS_p is the packing entropy for a reference additive-hard-sphere mixture, and ΔS_{na} is the correction to the entropy resulting from nonadditivity of the hard-sphere diameters. For ΔS_p we use the equation of state for additive hard sphere mixtures developed by Boublik, Mansoori, Carnahan, Starling, and Leland.³⁸⁻⁴⁰ Further, from the work of Ali *et al.* the nonadditivity correction takes the form (for an equiatomic composition) $\Delta S_{na} = -k_B \pi \rho \bar{\sigma}^2 \Delta \sigma g_{NiAl}(\sigma_{NiAl})$ in terms of the density (ρ) of the alloy, the radial distribution at the point of contact ($g_{NiAl}(\sigma_{NiAl})$), the average hard-sphere diameter [$\bar{\sigma} = (\sigma_{AlAl} + \sigma_{NiNi})/2$], and the deviation from additivity of hard-sphere diameters: $\Delta \sigma = \bar{\sigma} - \sigma_{NiAl}$. For liquid Ni, Al, and NiAl at 1900 K values of the geometrical quantities entering into the analytical hard-sphere entropy expressions described above have been determined from experimentally measured liquid densities (we emphasize that all AIMD simulations were performed at experimentally measured densities) and calculated radial distribution functions. For ΔS_p we compute a relatively large value of -0.42 k_B /atom. The magnitude of this term reflects the fact that the packing fraction in the NiAl alloy is considerably higher than the average of the values for pure Ni and Al. Due to the large negative deviation in Vegard's law for the liquid densities, the ideal-gas contribution to ΔS_{HS} is non-negligible: $\Delta S_{gas} = -0.1$ k_B /atom. Finally, owing to the nonadditive nature of the bond lengths in Ni-Al melts a significant correction to the additive-hard-sphere entropy is calculated: $\Delta S_{na} = -0.62 k_B$ /atom. When these three

contributions are combined, the following estimate for the configurational entropy results: $\Delta S_{\text{HS}} = -1.14 k_B/\text{atom}$. The sum of ΔS_{HS} and ΔS_{el} estimated above gives a value for the excess entropy of mixing equal to $-1.56 k_B/\text{atom}$. This value is comparable to the large excess entropies measured for Ni-rich alloys.^{4,5}

This research was supported by the Office of Science, Division of Materials Science, of the U. S. Department of Energy under Contract No. DE-AC04-94AL85000. Use was made of resources of the National Energy Research Scientific Computing Center, which is supported by the Office of Science of the Department of Energy under Contract No. DE-AC03-76SF00098.

- ¹M. Maret *et al.*, Phys. Rev. B **42**, 1598 (1990).
- ²A. B. Bhatia and D. E. Thornton, Phys. Rev. B **2**, 3004 (1970).
- ³L. D. Phuong *et al.*, Phys. Rev. Lett. **71**, 372 (1993); Mol. Simul. **20**, 79 (1997).
- ⁴I. Ansara *et al.*, J. Alloys Compd. **247**, 20 (1997).
- ⁵G. I. Batalin *et al.*, *Thermodynamics and the Constitution of Liquid Al Based Alloys* (Metallurgy, Moscow, 1983).
- ⁶A. I. Landa *et al.*, J. Phys.: Condens. Matter **3**, 9229 (1991); Yu. K. Kovneristyi *et al.*, J. Non-Cryst. Solids **117/118**, 589 (1990).
- ⁷A. Pasturel *et al.*, J. Phys. F: Met. Phys. **15**, L81 (1985).
- ⁸A. Pasturel, in *Statics and Dynamics of Alloy Phase Transformations*, Vol. 319 of *Advanced Study Institute, NATO Series B: Physics*, edited by P. E. A. Turchi and A. Gonis (Plenum, New York, 1994), p. 453.
- ⁹C. Colinet *et al.*, J. Phys.: Condens. Matter **1**, 5837 (1989).
- ¹⁰A. Pasturel *et al.*, J. Phys.: Condens. Matter **4**, 945 (1992).
- ¹¹G. Kresse and J. Hafner, Phys. Rev. B **47**, 558 (1993); **49**, 14 251 (1994).
- ¹²G. Kresse and J. Furthmüller, Comput. Mater. Sci. **6**, 15 (1996); Phys. Rev. B **54**, 11 169 (1996).
- ¹³D. Vanderbilt, Phys. Rev. B **41**, 7892 (1990).
- ¹⁴A. Pasquarello, K. Laasonen, R. Car, C. Y. Lee, and D. Vanderbilt, Phys. Rev. Lett. **69**, 1982 (1992).
- ¹⁵G. Kresse and J. Hafner, Phys. Rev. B **48**, 13 115 (1993); **55**, 7539 (1997).
- ¹⁶F. Kirchoff, J. M. Holender, and M. J. Gillan, Phys. Rev. B **54**, 190 (1996).
- ¹⁷F. Kirchoff, G. Kresse, and M. J. Gillan, Phys. Rev. B **57**, 10 482 (1998).
- ¹⁸G. A. de Wijs, G. Kresse, L. Voadlo, D. Dobson, D. Alfe, M. J. Gillan, and G. D. Price, Nature (London) **392**, 805 (1998).
- ¹⁹D. Alfe and M. J. Gillan, Phys. Rev. Lett. **81**, 5161 (1998); Phys. Rev. B **58**, 8248 (1998).
- ²⁰G. A. de Wijs, G. Kresse, and M. J. Gillan, Phys. Rev. B **57**, 8223 (1998).
- ²¹D. Alfe, M. J. Gillan, and G. D. Price, Nature (London) **401**, 462 (1999); **405**, 172 (2000).
- ²²D. Alfe, G. Kresse, and M. J. Gillan, Phys. Rev. B **61**, 132 (2000).
- ²³K. Seifert-Lorenz and J. Hafner, Phys. Rev. B **59**, 843 (1999).
- ²⁴O. Genser and J. Hafner, J. Phys.: Condens. Matter **13**, 981 (2001).
- ²⁵D. M. Ceperley and B. J. Alder, Phys. Rev. Lett. **45**, 566 (1980); J. P. Perdew and A. Zunger, Phys. Rev. B **23**, 5048 (1981).
- ²⁶H. J. Monkhorst and J. D. Pack, Phys. Rev. B **13**, 5188 (1976); **16**, 1748 (1977).
- ²⁷L. Verlet, Phys. Rev. **159**, 98 (1967).
- ²⁸S. Nosé, Mol. Phys. **52**, 255 (1984); J. Chem. Phys. **81**, 511 (1984).
- ²⁹A. F. Voter and S. P. Chen, in *Characterization of Defects in Materials*, edited by R. W. Siegel *et al.*, MRS Symposia Proceedings No. 82 (MRS, Pittsburgh, 1978), p. 175.
- ³⁰S. M. Foiles and M. S. Daw, J. Mater. Res. **2**, 5 (1987).
- ³¹M. Ludwig and P. Gumbsch, Modell. Simul. Mater. Sci. Eng. **3**, 533 (1995).
- ³²M. Asta *et al.*, Phys. Rev. B **59**, 14 271 (1999).
- ³³In the experimental results of Maret *et al.* (Ref. 1), the Ni-Ni partial pair correlation function displays a split first-neighbor peak. Such a feature was not observed in related experiments on Al₈₀Mn₂₀ alloys by the same investigators, and have not been reproduced in theoretical calculations for Ni₂₀Al₈₀ melts. The value of $R(\text{NiNi})$ reported in Table I corresponds to an average of the first two peak positions, as given by Maret *et al.*
- ³⁴As an independent check on the precision of calculated diffusion coefficients, we also derived values of D_{Ni} and D_{Al} by integrating calculated velocity-velocity correlation functions. The resulting diffusion coefficients are within ten percent of the results given in Table I: $D_{\text{Ni}}=0.26$ and $D_{\text{Al}}=0.44$, in units of $10^{-4} \text{ cm}^2/\text{s}$.
- ³⁵O. K. Andersen *et al.*, in *Application of Multiple Scattering Theory to Materials Science*, edited by W. H. Butler, P. H. Dederichs, A. Gonis, and R. Weaver, MRS Symposia Proceedings No. 253 (MRS, Pittsburgh, 1992), p. 37.
- ³⁶A. R. MacIntosh and O. K. Andersen, in *Electrons at the Fermi Surface*, edited by M. Springford (Cambridge University Press, Cambridge, England, 1980).
- ³⁷G. Grimvall, *Thermophysical Properties of Materials* (North-Holland, Amsterdam, 1999).
- ³⁸N. F. Carnahan and K. E. Starling, J. Chem. Phys. **51**, 635 (1969).
- ³⁹T. Boublik, J. Chem. Phys. **54**, 1523 (1971).
- ⁴⁰G. A. Mansoori *et al.*, J. Chem. Phys. **54**, 1523 (1971).
- ⁴¹I. Ali *et al.*, J. Non-Cryst. Solids **250-252**, 360 (1999).